

EROSION PROCESSES OF NATURAL RIVER BANK

by

Shoji Fukuoka

Professor, Department of Civil and Environmental Engineering

Faculty of Engineering, Hiroshima University

Hiroshima, Japan

ABSTRACT

The present study deals with erosion process of natural bank with strata and makes it possible to estimate the rate of bank erosion. Channels were dug on the flood plain of the Ara River. Erosion process was found to be composed of three stages: erosion of lower non-cohesive layer of bank, collapse of overhanging upper cohesive layer in tension and the breakup and transport of the collapsed soil mass by the flow. Further, the estimating method was proposed for collapse of the upper silty soil and transport of the collapsed soil mass by dynamical considerations.

1. INTRODUCTION

Much research has been performed on issues concerning bank erosion, and most analysis based on the hydraulic experiment technique primarily involves research on the mechanisms of erosion in banks comprised of non-cohesive soils. (1) (2) However, the natural bank generally has a layered structure comprised of sand, silt, clay and a variety of other types of soil, and hence the erosion of non-cohesive soil does not sufficiently reflect the erosion of natural banks. Therefore, it is of the utmost importance that examinations involving bank erosion be performed in the river. Fujita and Muramoto (3) have, since 1980, observed erosion in the Uji river over the passage of time and have discussed erosion rates. Hasegawa (4), in addition to his theoretical examination of bank erosion, has also achieved important results on the relationship between the coefficient of bank erosion and bank soil in meandering rivers in Hokkaido. Overseas, meanwhile, field surveys are being energetically performed, primarily by geologists. (5)(6) However, while these researches have helped to explain the fundamentals of the phenomenon of erosion, it has not yet reach the stage where it can be used in designing the longitudinal and cross-sectional profile of channels, taking account of soil structures and flood hydraulics. Therefore, for this paper we dug several channels in the flood plain (formed through natural sedimentation) of a river and performed erosion experiments on natural banks with different soil structures in order to extensively investigate the mechanism and process of bank erosion and estimate the erosion rate of bank. (7)

2. FIELD EXPERIMENTS ON BANK EROSION IN FLOOD CHANNELS OF THE ARA RIVER

In order to understand the erosion characteristics of a natural bank, it is necessary to quantify the relationship between flow and channel conditions and the position and thickness of the layer, which has low erosion resistance. To do this, we dug channels with a curvature radius of 15 m, a length of 30 m, a width of 0.9 m, a depth of 0.5 m, and a bed slope of 1/100 in the flood channel of the left bank of the Ara river near the 64-km point. Discharge was $0.14 \text{ m}^3/\text{s}$, average depth 0.15 m, and initial average velocity 1.2 m/s. Total flow time was 66 minutes, but midway the flow was stopped to measure changes in bank profile, velocity distribution, etc., over the passage of time. (see photo 1)

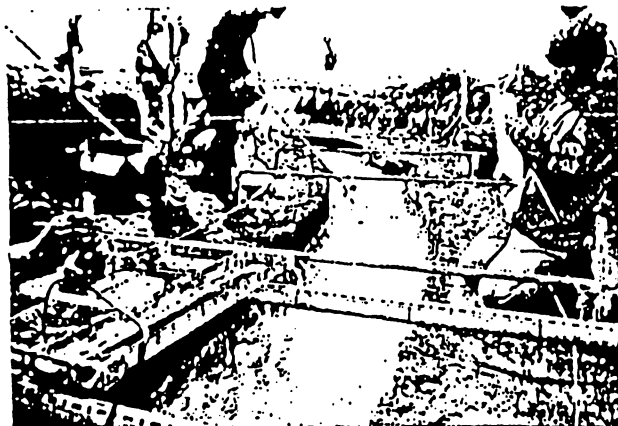


Photo 1: Field experiment

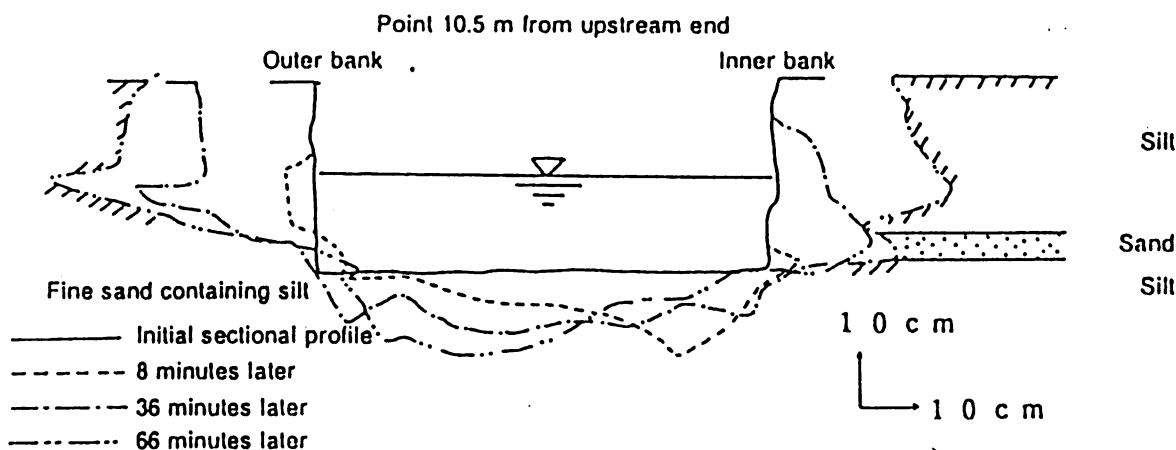


Fig. 1: Bank erosion conditions

The bank here had a very clear layered structure comprised of layers of sand, silt, clay, and a mixture of all three. Figure 1, the bank erosion conditions at a typical section (at the point 10.5 m from the upstream end), shows that the outer bank is comprised of fine sand containing silt, while the inner bank is comprised of alternating layers of silt and sand. It also shows that on the inner bank, the underwater sand layer began eroding first, after which the high-cohesion silt layer above the sand layer collapsed.

Comparing banks in 36 minutes and 66 minutes, one can see that the collapsed soil mass in the inner bank was limiting further erosion in the sand layer by covering its front surface. In the same manner the underwater portion of the outer bank began eroding first, after which the portion of the bank above the water surface began overhanging and eventually collapsed. This collapsed soil mass had lower cohesion than that of the inner bank and therefore was quickly disintegrated by the current. As a result, it was immediately transported away with nothing left behind. This type of collapse was observed several times during the course of the experiment, and it would seem that bank erosion

progresses through repeated collapsing during flooding.

The above suggests that the process of erosion in natural banks is, as shown in Figure 2 comprised of three stages: erosion of the lower less-cohesive layers (stage 1), collapse of the overhanging upper cohesive layer (stage 2), and the break-up and transport of the collapsed soil mass (stage 3). As erosion of the less cohesive layer progresses, the upper layer of banks overhangs. Velocity below this overhang then decreases and the rate of erosion in this layer is reduced.

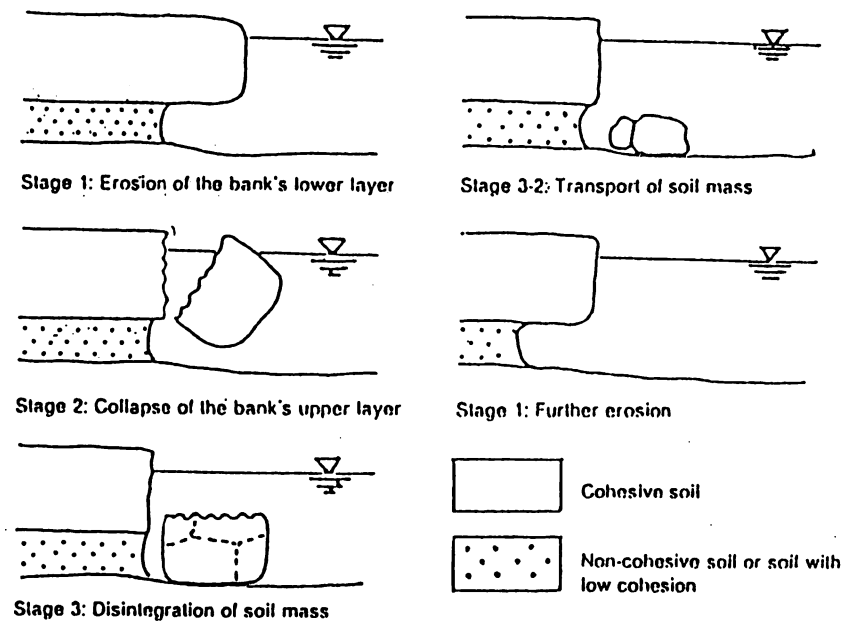


Fig. 2: The erosion process in a natural bank

The extent of this reduction in erosion rate depends on the length of the overhang, while the maintainable length of the overhang depends, in turn, on the cohesion of the soil layer. The collapsed soil mass settles on the river bed near the bank and, until it is transported away, makes it difficult for further erosion in the sand layer to occur. Hence, the time required for the soil mass to be transported away results in further erosion in the sand layer being postponed.

Figure 3, an example of changes over time in the amount of bank erosion measured, shows that collapse (i.e., stage 2) results in the rapid progression of erosion.

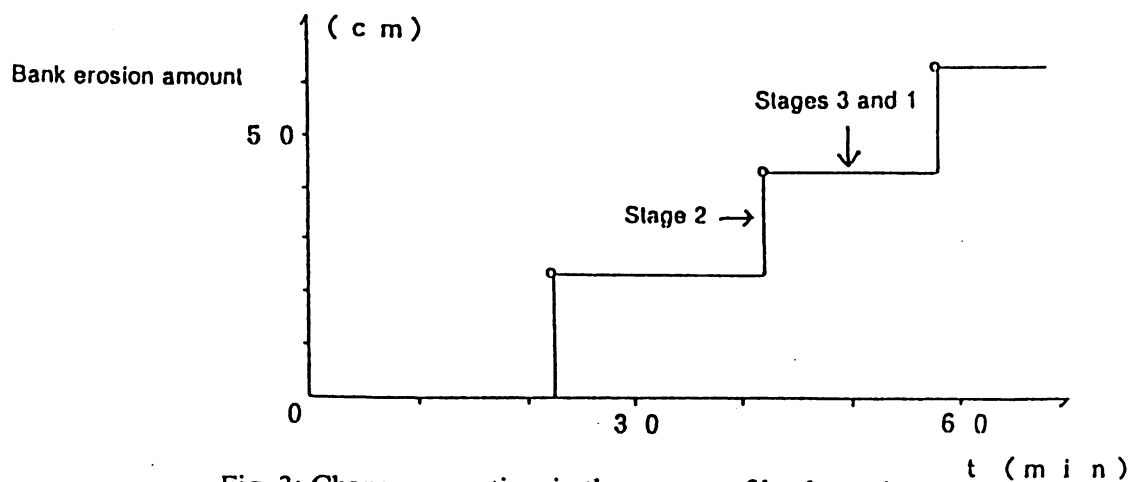


Fig. 3: Changes over time in the amount of bank erosion

After determining, in this manner, the mechanism of bank erosion to a certain extent, we attempted a quantification of the rate of erosion throughout a natural bank. To do this, we decided to investigate

each stage separately, then integrate the results for each. The following sections deal primarily with the stages of collapse and transport. Essential to a discussion of the rate of erosion in the entire bank is an estimate of the delay in erosion caused by adding cohesive soil to the materials of which the bank is comprised.

3. INVESTIGATION THE COLLAPSE STAGE

Because it is the soil's tensile stress that resists collapse right until it occurs, determining the tensile strength of the high-erosion-resistance upper layer soil mass would make it possible to estimate the critical protrusion length of stage 2. With this objective, we performed a field experiment on the tensile strength of soil at a field location where an overhang had been formed inside the channel. In it, for each soil material we measured the critical length of the protrusion (i.e., the maximum maintainable length). The steps of the experiment are as follows (see Photo 2).

First, the lower layer of the bank was dug out to create an overhang of a consistent thickness and with the crown as its surface. Next, two vertical grooves were gently cut in the bank in order to release the stress acting on the adjacent soil. We then continued digging similar grooves until the soil mass in our experiment collapsed from the bending moment caused by its own weight.

After this, measuring the weight and size of the collapsed soil mass as well as the surface area of the breaking surface, we calculated the tensile strength that had been acting on the breaking surface in accordance with the dynamics of cantilever beams. We have hypothesized that the tensile strength that was acting on the breaking surface at the time of collapse has a distribution like that shown in Figure 4. H (cm) is the thickness of the protrusion, L (cm) its length, and B (cm) its width. We assume that the external force moment caused by W , the protrusion's own weight (kgf), and the resistance moment that occurs on the breaking surface balance out and reach tensile strength (kgf/cm^2) T_0 at the upper edge of the breaking surface. The following equation for this instant holds.

$$W \cdot L/2 = H^2 T_0 B / 6 \quad (1)$$

This equation is used to express the tensile strength of the soil with the following equation.

$$T_0 = 3WL/H^2 B \quad (2)$$



Photo 2: Soil mass collapse in the experiment

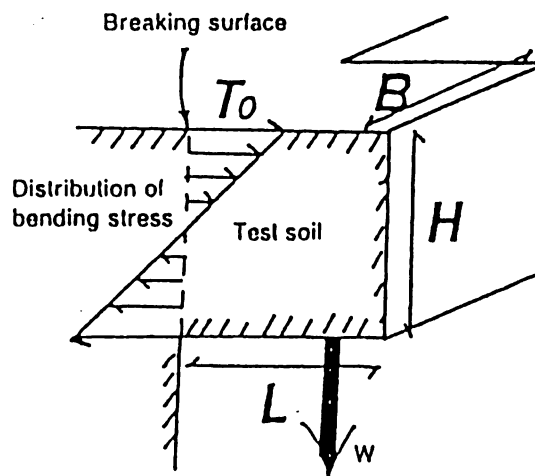


Fig. 4: The distribution of stress acting on the breaking surface

The tensile strengths calculated with equation (2) are shown in Table 1.

Table-1: Results of experiment on the tensile strength of different types of soil

Place	Soil	H (cm)	L (cm)	B (cm)	W (kgf)	W/B (kgf/cm)	To (kgf/cm ²)
Point 9 m from upstream end	Silt (containing sand)	12.5	21.0	23.0	4.70	2.04 x 10 ⁻¹	8.25 x 10 ⁻²
		14.5	16.0	14.0	5.08	3.63 x 10 ⁻¹	8.28 x 10 ⁻²
Point 14 m from upstream end	Silt (containing clay)	13.8	18.0	10.0	3.74	3.74 x 10 ⁻¹	1.06 x 10 ⁻¹
		10.0	17.0	9.0	1.84	2.04 x 10 ⁻¹	1.04 x 10 ⁻¹
Point 30 m from upstream end	Fine sand	10.0	4.5	10.0	0.642	6.42 x 10 ⁻²	8.67 x 10 ⁻³
		10.0	3.5	10.0	0.499	4.99 x 10 ⁻²	5.25 x 10 ⁻³

These calculated results show that the values for the tensile strength of soil with a high erosion resistance obtained in each experiment are nearly constant. Transforming equation (2) results in equation (3), where γ (kgf/cm³) is soil density.

$$L = (T_o \cdot H/3\gamma)^{1/2} \quad (3)$$

This equation is used to determine the critical overhang length by assigning values for the thickness of the overhang layer, soil density, and soil tensile strength.

Figure 5 show the critical overhang length calculated using the cross sections obtained in water flow experiments and the values for T_o , H and γ obtained in the soil experiments. This figure shows that critical overhang length is nearly the same as the actual overhang length just prior to collapse, and that it is therefore possible to predict stage 2 with equation (3).

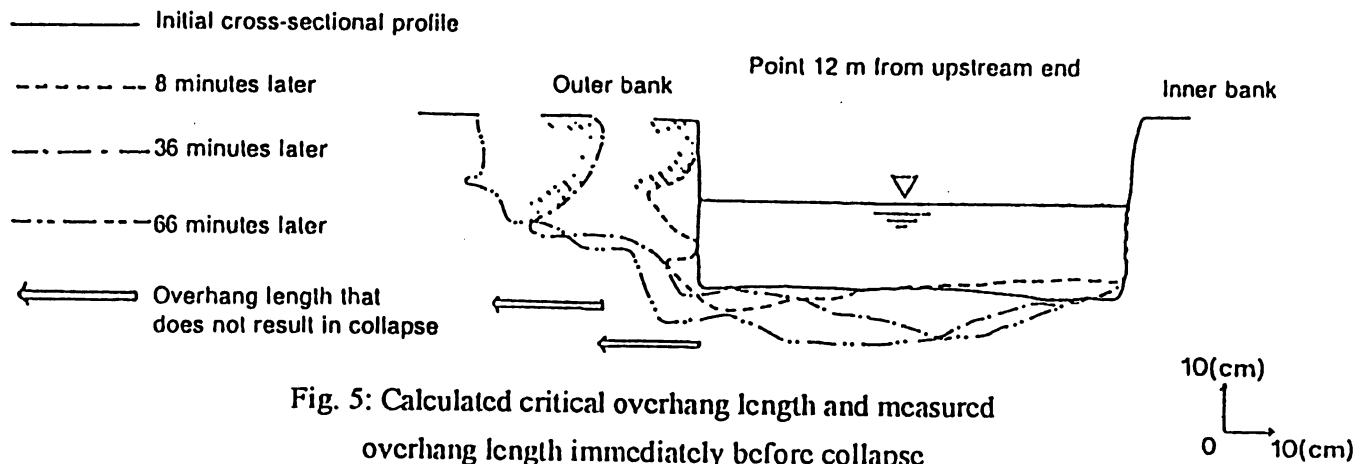


Fig. 5: Calculated critical overhang length and measured overhang length immediately before collapse

Next, to investigate the size of protrusions for which equation (3) can be applied, we performed tensile strength experiments on overhangs 10, through 150 centimeters in size (H). The soil unit volume weight used was $\gamma=1.85 \times 10^{-3}$ kg/cm³. When a soil tensile strength of $T_o=0.143$ kgf/cm² is selected at this time, equation (3) nearly corresponds with the observed results of lengths (L) by practical collapse heights (H) (see Figure 6).

4. THE TRANSPORT OF COLLAPSED SOIL MASS

In order to determine the amount of time required for the collapsed soil mass to be transported (stage 3), we performed a soil mass transport experiment.

For this experiment we used a straight channel 16 m long, 1 m wide, and 0.4 m deep. The cohesive soil specimens used were taken from an actual river site.

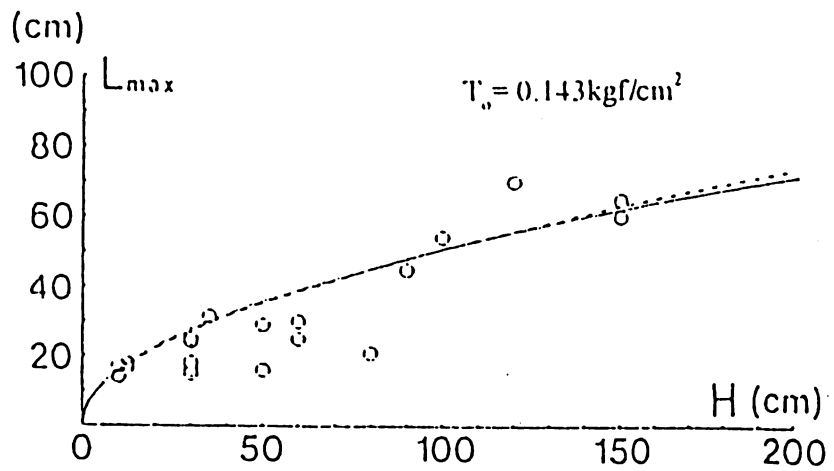


Fig. 6: Results of tensile strength experiment in which the scale of test soil was changed

In the experiment we measured time and weight (converting to volume using the unit volume weight) of soil masses placed in a current and transported by the water, while at the same time also measuring discharge, velocity distribution, and water surface slope.

The soil masses used were comprised of silt and clay containing silt; the largest was roughly 30 x 30 x 25 cm in size, while the smallest was 7 x 7 x 7 cm. Velocity was changed within the limits of 60 and 85 cm/s. Some soil masses placed in the current rolled away while others did not; those that rolled away were considered as having been transported. Those that did not roll away would gradually lose volume, then be transported after they reached a certain size. Silt soil masses would sometimes be gradually transported in a manner that fragments 5 to 6 cm in size separate from the surface and come to piece, while other silt soil masses would rapidly break apart into several large pieces and then be transported. Soil masses comprised of clay mixed with silt were gradually worn away at the surface and eventually transported, but sometimes, when the soil structure contained heterogeneous portions, this caused the entire soil mass to rapidly break apart and be transported. This shows that the transport of a soil mass is comprised of two stages: disintegration, the stage wherein a large soil mass is reduced in size by the current; and transport, the stage wherein a reduced soil mass is carried away by the current.

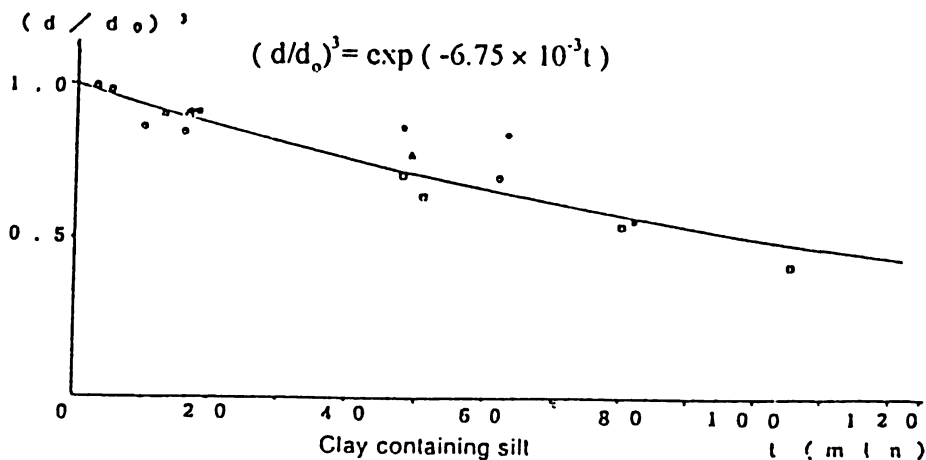


Fig. 7: Changes over time in the volume of the soil mass (clay containing silt)

Let us first consider the first stage, disintegration. Figures 7 and 8 show how a soil mass comprised of clay containing silt and silt is reduced in size. The horizontal axis represents time, while the vertical axis represents the ratio between initial volume and the volume after the passage of a certain amount of time. The reason that the former shows less dispersion than the latter is that while clay containing silt is gradually worn away at the surface, it is more common for soil masses comprised of silt to be broken apart by the current and reduced in size.

Through this experiment we are able to approximate with the following expression the stage wherein a soil mass is reduced in size.

$$d^3 = d_0^3 \exp(-\alpha t) \quad (4)$$

As α is determined by shear stress τ and soil cohesion c , it is called the soil disintegration coefficient. Using the results from this experiment to determine the value of α when $\tau = 35.2 \text{ g/s cm}^2$ results in $\alpha = 6.75 \times 10^{-3}$ (clay containing silt) and $\alpha = 2.16 \times 10^{-2}$ (silt). In the future we must investigate the relationship between α , τ and c further.

Next, we shall consider the second stage, transport. Here we assume a cube-shaped soil mass. The forces acting on the cube are gravity, drag and lift caused by the current (see Figure 9). We also assume that all these forces act on the object's center of gravity. The moment of the gravity, drag and lift around point A in the critical state is as follows.

$$\begin{aligned} W' \sin\varphi \cdot OA - L \sin\theta \cdot OA - \\ D \cos\varphi \cdot OA = 0 \end{aligned} \quad (5)$$

Solving equation (5) with respect to soil mass size d , we arrive at equations (6).

$$d = k \cdot (R^{1/3}/n^2 g) \cdot \tau \cdot (C_D + C_L \tan\varphi) / 2 (\sigma - \rho) g \tan\varphi \quad (6)$$

This makes it possible to determine the relationship between τ and soil mass size d . k is the correction factor, derived by assuming, for instance, that the soil mass is cubic. Plotting data obtained in the experiment concerning the relationship between τ and d produces Figure 10.

When using the values $C_D = 1.36$, $C_L = 0.18$, $\varphi = 45$ degrees, $\sigma = 1.85 \text{ g/cm}^3$, $\rho = 1.00 \text{ g/cm}^3$, and $g = 980 \text{ cm/s}^2$ and substituting into equation (6), the following value for k is obtained: $1.82 < k < 2.06$. The value of k is generally considered to be around one, and the above values are thought to be within the range of error.

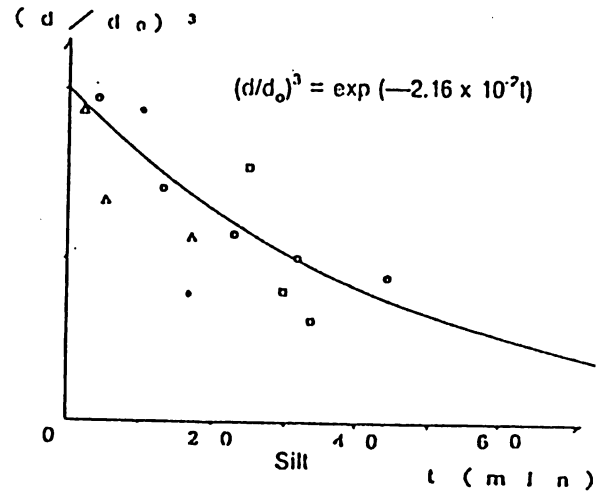


Fig. 8: Changes over time in the volume of the soil mass (silt)

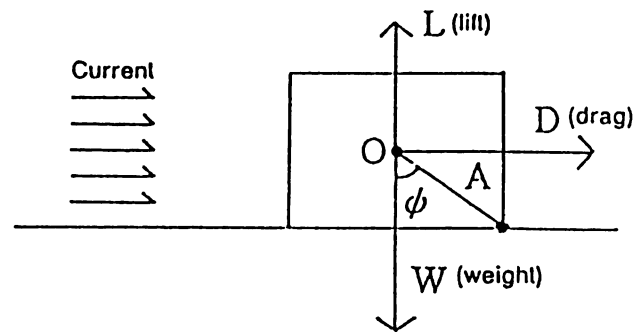


Fig. 9: Forces acting on the soil mass

Here, we assume that a single soil mass lies on a flat bed: a single soil mass in such conditions is more easily transported than closely-grouped multiple soil masses. Therefore, future investigations are necessary to determine the extent to which the sheltering effect of other soil masses has on the transport stage.

5. CONCLUSION

Erosion experiments performed with a natural-sedimentation river bank show that the erosion of an entire natural bank progresses through repetition of a three-stage process: erosion, collapse and transport.

This paper also discussed how to predict the critical overhang length at which collapse occurs in addition to the mechanism whereby a collapsed soil mass is transported and how to determine the time required for the soil mass to be transported

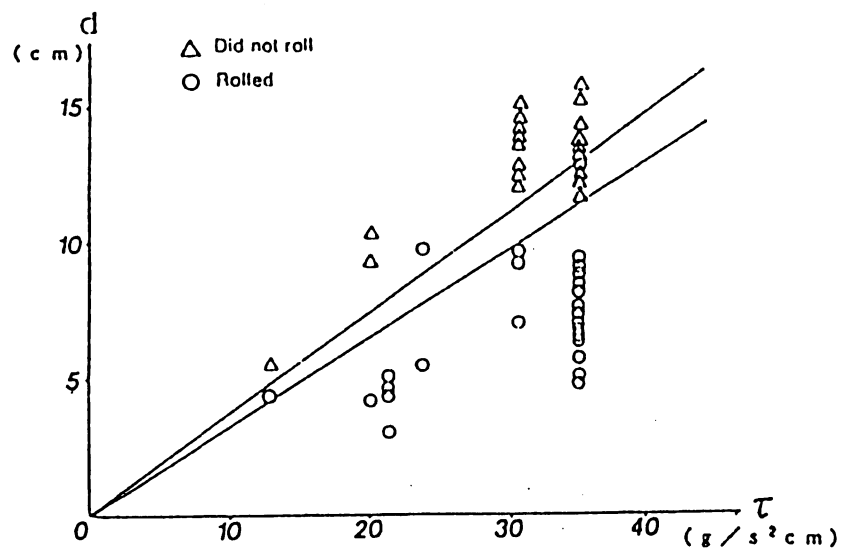


Fig. 10: The transport threshold of soil masses

REFERENCES

- 1) HIRANO, M.: River-Bed Variation with Bank Erosion, Proc. of the JSCE, No. 210, pp. 13-20, 1973 (in Japanese).
- 2) FUKUOKA, S., and YAMASAKA, M.: Shear Stress Distribution on a Continuous Boundary and Widening Process of a Straight Alluvial Channel, Proc. of the JSCE, No. 351/II-2, pp. 87-96, 1984 (in Japanese).
- 3) FUJITA, Y., MURAMOTO, Y. and MIYASAKA, H.: Observation of River Bank Erosion, 6th Congress APD-IAHR Proceedings, Vol. II-1, River Hydraulics, pp. 123-130, 1990.
- 4) HASEGAWA, K.: Universal Bank Erosion Coefficient for Meandering Rivers, Journal of Hydraulic Engineering, ASCE, Vol. 115, No. 4, pp 1989.
- 5) THORNE, C.R.: Process of Bank Erosion in River Channels. University of East Angeli (Ph.D. thesis) 445p., 1978.
- 6) THORNE, C.R. and TOVEY, N.K.: Stability of Composite River Banks, Earth Surface Process and Landforms, Vol. 6, pp. 469-484, 1981.
- 7) FUKUOKA, S.; KOGURE, Y., SATO, K. and DAITO, M.: Erosion Processes of River Bank with Strata. Proc. of Hydraulic Engineering. JSCE, Vol. 37, pp. 643-648, 1993 (in Japanese).